Landscape and Urban Planning 209 (2021) 104046

Contents lists available at ScienceDirect

Landscape and Urban Planning

journal homepage: www.elsevier.com/locate/landurbplan

Research Paper

Small vegetated patches greatly reduce urban surface temperature during a summer heatwave in Adelaide, Australia

Alessandro Ossola [a,b,c,*], G. Darrel Jenerette [d], Andrew McGrath [e], Winston Chow [f], Lesley Hughes [g], Michelle R. Leishman [g]

[a] Department of Biological Sciences, Macquarie University, North Ryde, NSW 2109, Australia
[b] Department of Plant Sciences, University of California, Davis 95616, CA, USA
[c] School of Ecosystem and Forest Science, University of Melbourne, Richmond, VIC 3121, Australia
[d] Department of Botany and Plant Sciences, University of California Riverside, 3203 Batchelor Hall, Riverside, CA 92506, USA
[e] Airborne Research Australia, PO Box 335, Salisbury South, SA 5106, Australia
[f] School of Social Sciences and Office of Core Curriculum, Singapore Management University, 90 Stamford Road, Level 4, Singapore 178903, Singapore
[g] Department of Biological Sciences, Macquarie University, North Ryde, NSW 2109, Australia

HIGHLIGHTS

- Cooling benefits by urban vegetation are greater at land unit than the suburb scale.
- Vegetation provides greater cooling benefits to suburbs further from the coast.
- Private green spaces are disproportionally important for urban heat mitigation.
- Yards and trees are an overlooked asset for localised climate change adaptation.
- People can adapt to heat when and where needed the most; during heatwaves and near home.

ARTICLE INFO

Keywords:
Extreme heat
Climate change
Adaptation
Public health
Risk planning

ABSTRACT

As the global climate warms, cities worldwide face more frequent and extreme heatwaves. These events can affect human health and decrease liveability. While the mitigating effects of vegetation on land surface temperature (LST) are well characterised at large spatial scales and during typical weather conditions, the cooling benefits that urban greening can provide at local scales, particularly during summer heatwaves, are poorly quantified.

We quantified LST variation across an urban landscape to assess relationships with land use and vegetation cover from land unit (average ~ 460 m^2) to suburb scale (~1.66 km^2) under extreme summer heat conditions. High resolution (2 m), day- and night-time LST was measured at the peak of a heatwave event, after three consecutive days with air temperature exceeding 40 ℃, by flying an aircraft fitted with a thermal imager over 90 suburbs in Adelaide, Australia. Daytime, night-time, and diurnal range LST distributions were related to measures of land use, vegetation cover (i.e., tree, grass) and urban morphology at both the suburb and land unit scale.

At the suburb scale, vegetation cover did not affect LST. However, at the land unit scale, tree canopy cover, and to a lesser extent grass cover, decreased local LST by up to 6 ℃ during the day, but not at night. Overall night-time LST was poorly predicted by the land use and land cover predictors. Moving inland from the coast, small vegetation patches, mostly contained in yards and gardens, was associated with the greatest localised LST reductions in the hotter inland suburbs. LST within land units was further decreased during the day when vegetation was present within 30 m buffers around each land unit, suggesting a moderate landscape cooling effect on LST.

* Corresponding author at: Department of Biological Sciences, Macquarie University, North Ryde, NSW 2109, Australia.
E-mail addresses: alessandro.ossola@mq.edu.au, aossola@ucdavis.edu.au (A. Ossola), Darrel.Jenerette@ucr.edu (G.D. Jenerette), andrew.mcgrath@airborneresearch.org.au (A. McGrath), winstonchow@smu.edu.sg (W. Chow), lesley.hughes@mq.edu.au (L. Hughes), michelle.leishman@mq.edu.au (M.R. Leishman).

https://doi.org/10.1016/j.landurbplan.2021.104046
Received 10 June 2020; Received in revised form 12 January 2021; Accepted 15 January 2021
Available online 30 January 2021

Our results suggest that even small urban vegetation patches can be managed to provide substantial heat mitigation during increasingly frequent summer heatwaves, particularly around the residential environments where people live.

1. Introduction

The average global temperature is now more than 1 °C above pre-industrial levels and the years 2015–19 were the five warmest on record (WMO, 2019b). The global warming trend is associated with significant increases in the frequency and intensity of extreme weather events, including heatwaves, with the latter defined as periods "*of at least three days where the combined effect of excess heat and heat stress is unusual with respect to the local climate*" (Nairn and Fawcett, 2013).

Heatwaves have significant impacts on human health, biodiversity, infrastructure and economies (Gasparrini et al., 2015; Watts et al., 2018). Extreme heat can exacerbate existing health issues, such as cardiovascular and respiratory disease, and is associated with increased hospital admissions, psychological stress and aggressive behavior (Harlan et al., 2013), as well as excess mortality (Robine et al., 2008; Shaposhnikov et al., 2014). From 2000 to 2016, the number of people exposed to heatwave risk globally is estimated to have increased by around 125 million, with the average length of individual heatwave events increasing by 0.37 days, compared to 1986 – 2008 (Watts et al., 2018). Worldwide, an estimated 175 million people were exposed to more than 600 heatwaves in 2015 alone. The recently released *United in Science* report, compiled under the auspices of the *World Meteorological Organisation* to coincide with the *United Nations Climate Action Summit* in 2019, reported that heatwaves were the "*deadliest meteorological hazard*" in the 2015–2019 period, affecting all continents, with national heat records set in many regions (WMO, 2019a). The impacts of heatwaves under a future 2 °C warming scenario are projected to be considerably greater than those for 1.5 °C (IPCC, 2018). One modelling study concluded that 13.8% of the world's population would be exposed to "*severe heatwaves*" at least once every 5 years with warming of 1.5 °C, but 36.9% at 2 °C, a difference of approximately 1.7 billion people (Dosio et al., 2018). As the world's cities house more than 55% of the current global population, with this figure potentially increasing to nearly 70% by 2050 (United Nations, 2018), the interactive effects of future climate change and urbanisation will increase risks associated with extreme urban heat (Rogers et al., 2018).

Heat exposure risk during heatwaves can be further exacerbated in some urban areas as these can be relatively warmer than surrounding areas - the Urban Heat Island (UHI) effect - due to modifications of the urban land surface and anthropogenic heat from energy use (Oke et al., 2017). Overall, the mean annual air temperature in a large urban area may be 1–2 °C warmer than the surrounding *peri*-urban area, and up to 12 °C warmer on calm, clear nights (American Meteorological Society, 2020). The Surface Urban Heat Island (SUHI) can be quantified by measuring land surface temperatures (LST) of composite materials at the urban surface and comparison with rural or non-urban surfaces (Oke et al., 2017). Differences in composite urban vs. non-urban LST are driven by spatio-temporal variations in the surface energy balance, namely in radiative, conductive and turbulent fluxes. Some urban features can locally accumulate large amounts of heat during the day, often increasing urban LST well above 60 ℃ on hot summer days, depending on the thermal properties of their materials (Bonan, 2000). Across coastal cities, where much of the global urban population resides (Threlfall et al., 2021), lake or marine effects can further lead to steep gradients in LST at the city scale (Declet-Barreto et al., 2016; Tayyebi and Jenerette, 2016). This is particularly true in Australian cities which are affected by synoptic conditions such as warm air from inland deserts and cool sea breezes (Khan et al., 2021).

Recent large-scale assessments of heat across urban landscapes found that greener suburbs, characterised by higher forest cover and lower impervious surface area, often have lower LST compared to areas with lower tree cover (Imhoff et al., 2010; Manoli et al., 2019; Tayyebi and Jenerette, 2018). Solar energy is used by plants for photosynthesis and related processes (Bonan, 2000). Greater plant and leaf biomass can lead to a larger latent heat flux and higher transpiration, and reduce surface resistance to evapotranspiration (Hulley et al., 2019). In this way, tree canopies can often maintain a daytime surface temperature close to that of the surrounding air (Mildrexler et al., 2011). Vegetation affects heat fluxes and microclimate at a location depending on its overall structural and spectral properties, such as leaf cover and seasonality, roughness and albedo (Hulley et al., 2019). Urban trees and tall vegetation can also shade infrastructures and buildings, avoiding heat accumulation within these features during the day and reducing urban LST (Bonan, 2000). Conversely, during the night, the urban forest can trap heat, causing localised increments of air and surface temperature in some locations (Ziter et al., 2019). These mechanisms collectively mean that urban vegetation and green-infrastructure (e.g., green roofs and walls) are increasingly being suggested as an effective and relatively inexpensive adaptation strategy to decrease urban heat, particularly in the context of the risks posed by ongoing climate change (Bowler et al., 2010; Jenerette et al., 2011), although the magnitude and timing of localised cooling effectiveness is uncertain, especially in relation to high intensity heat waves.

Studies investigating urban heat and LST to date have been primarily conducted at a relatively coarse spatial resolution (60–100 m from Landsat and ASTER satellite platforms) that is ineffective for capturing the fine-scale thermal structure and granularity of urban landscapes (Declet-Barreto et al., 2016; Zhou et al., 2017). Similarly, urban canopy cover assessments often rely on coarse spatial data as well as proxies, such as the Normalised Difference Vegetation Index (NDVI) (Declet-Barreto et al., 2016; Imhoff et al., 2010), that make little distinction between urban forest types and structures (e.g., trees vs herbaceous cover). This greatly limits our understanding of the local relations between urban heat and urban vegetation, as both are highly variable in their spatial distribution across cities and urban landscapes (Jenerette et al., 2016). Urban vegetation cover and structure, for instance, can dramatically vary at a fine-scale based on urban morphology, land use, socio-economic factors and people's preferences (Ossola et al., 2019a, 2019b). In this way, it is reasonable to expect the moderating effects of urban vegetation cover on LST to be also highly localised and spatially variable.

Fine-scale assessments of the relationship between urban vegetation and extreme heat across an entire urban landscape are scant (Bartesaghi-Koc et al., 2018). Similarly, there is little available information about multi-scalar effects of urban vegetation in moderating LST during heatwaves i.e. comparing differences between smaller land units such as residential yards managed by residents, to larger units such as parks and streetscapes managed by public authorities. There is limited knowledge, therefore, as to how even small-scale and localised greening interventions, such as vegetated patches of a few dozens of square meters, might compound and extend their cooling effects at the parcel (hundreds of m^2), suburb (few km^2), landscape (dozens of km^2) and city-scale (hundreds of km^2) (Bartesaghi-Koc et al., 2018). Conversely, it is not fully understood how the larger urban forest might contribute to local cooling benefits at the land unit scale and how these benefits could extend from vegetation patches into adjacent areas (i.e., buffers) (Jenerette et al., 2016; Ziter et al., 2019).

Precise measurements of urban heat during extreme weather events have been challenging because of the stochasticity of these events and current technological limitations (e.g., long satellite revisit times, cloud

cover, low sensor resolution, etc.). Where satellite-based LST data is available during extreme heat anomalies, they are usually limited to either day or night overpasses, thus limiting our capability to investigate fine-scale diel LST variation and the capacity of urban thermal landscapes to cool off during the night when under extremely hot conditions. This is important because large temperature variations, particularly at a higher temperature range, can further exacerbate heat stress in humans (Petitti et al., 2016).

On the other hand, where more precise field-based measurements of urban heat have been performed at a local scale (i.e., few km^2), they have generally focused on one or a few suburbs or specific land uses, such as urban parks, that are an imperfect representation of the thermal complexity of a metropolis (Bonan, 2000; Bowler et al., 2010). Fewer studies measuring LST of grass and short vegetation cover have been performed compared to those investigating single trees or entire urban forests (reviewed in Bowler et al. (2010)), and little information exists on how LST varies across land units (e.g., yards, building rooftops, land parcels). In this way, the localised cooling benefits that urban vegetation as a whole can provide across entire cities are generally poorly quantified, particularly i) *when* these benefits are needed the most, i.e., during heatwaves, hot spells and extremely hot days, and ii) *where* these benefits are needed the most, i.e., locally in the residential parcels where most people live.

To address these knowledge gaps, we measured urban LST within 90 suburbs across the coastal city of Adelaide, Australia during a summer heatwave, at the end of three consecutive days with maximum air temperature $\geq$ 40 ℃, which exceeds by more than 10 ℃ the average maximum air temperature (29.5 ℃) historically recorded for this period (Bureau of Meterology, 2019). The onset and development of this 3-day heatwave event was constantly monitored in order to fly a dedicated aircraft twice during the peak of the event and measure daytime and nighttime LST at a very fine spatial resolution (2 m). The day flight allowed us to also collect spectral data of the urban vegetation to create a high resolution (30 cm) map of vegetated patches (e.g., single tree canopies, small herbaceous patches in yards). The LST data collected during the heatwave has a resolution between 13 and 900 times greater than previously collected datasets, enabling a much more precise measurement of LST associated with relatively small urban features, urban vegetated patches and land use units (e.g., residential yards, rooftops, etc.) subjected to extreme heat conditions.

In addressing this overall goal, we firstly measured how urban land surface temperatures, recorded during the day, night and their differential (LST_{day}, LST_{night} and LST_{Δ}, respectively), vary during a heatwave at the suburb and land unit scale. We further assessed the extent to which non-vegetated and vegetated patches within suburbs and land units affect local urban LST during a heatwave. We finally quantified the landscape effect of the vegetation around each land unit at decreasing LST during a heatwave.

We anticipated that, at the larger city scale, LSTs would increase with the distance from the maritime coast west of Adelaide, as observed in other cities under ordinary weather conditions (Declet-Barreto et al., 2016; Tayyebi and Jenerette, 2016). We further expected that, on a smaller local scale, vegetation might decrease LST within local buffers adjacent to each land unit, as observed elsewhere for air temperature under ordinary weather conditions (Ziter et al., 2019).

2. Materials and methods

2.1. Study area

Adelaide is located on the coast in the south-central portion of the Australian continent, bordering its central steppe and desert. The climate is hot temperate with dry summers (mean annual maximum temperature = 21.6 °C [1955–2019]; mean annual rainfall = 439.9 mm, (Bureau of Meteorology, 2019)). Adelaide suffers from a moderate boundary layer UHI with nighttime rural–urban differences in air temperature peaking at 5.9 °C (Soltani and Sharifi, 2017). Australia is considered one of the most vulnerable developed countries to the impacts of climate change (Reisinger et al., 2015). The number of record hot days in Australia has doubled since the 1960s and heatwaves have become longer, hotter and more intense (Cowan et al., 2014; Perkins and Alexander, 2012). Among Australia's state capitals, Adelaide is severely affected by frequent heatwaves with the mean annual number of hot days (greater than 35 ℃) increasing from 17.5 [1961–1990] to 25.1 [2000–2009] (Steffen et al., 2014), and further projected to increase up to 51 days by 2090 under current greenhouse gas emission trajectories (Ogge et al., 2019). Increasing heatwave intensity has been particularly pronounced in Adelaide, where the peak heatwave air temperature in the period 1980–2011 was 4.3 °C higher than that for the period 1950–1980 (Steffen et al., 2014). The historical trend of extreme heat events in Adelaide culminated in 2019 when the hottest air temperature ever recorded in an Australian state capital reached 46.6 ℃ on January 24th (Commonwealth of Australia, B. o. M., 2019). Projections of extreme temperatures in Australia do not scale linearly with mean global warming and modelling indicates that major Australian cities could experience extreme air temperatures exceeding 50 °C under 2 °C of global mean warming (Lewis et al., 2017).

Heatwaves are Australia's deadliest weather-related hazard, causing more deaths since 1890 than bushfires, cyclones, earthquakes, floods and severe storms combined (Coates et al., 2014). In eastern Australian cities, for example, mortality has been observed to increase when the maximum air temperature exceeds 28–30 °C (Guest et al., 1999). Over the past four decades there has been a steady increase in the number of deaths of Australians in summer, compared to those in winter, indicating that warming increases mortality rates (Bennett et al., 2014). Currently, the greater Adelaide area has the highest rate of heat-related deaths among the country's capital cities (Longden, 2018).

The study area (~149 km^2) encompasses three municipalities (Port Adelaide-Enfield, Charles Sturt and West Torrens) and 90 suburbs nested between the city center and its maritime coast on the west (Fig. 1A and SI Appendix). Suburbs are located in a coastal plain (0–25 m a.s.l.) at a distance from the coast between 0 and 8 km. The study area is densely populated (population = 300,377 people, population density = 1,635 people km^{-2}, house tenant occupancy = 29.31%, (Australian Bureau of Statistics, 2017)), and is expected to further increase its population due to planned urban densification and renewal aimed at reducing urban sprawl around the greater Adelaide metropolitan area (Government of South Australia, 2017). Despite the high population, several suburbs selected for the study have a diverse composition of up to 12 land uses comprising commercial, mixed-use and industrial land that are less populated than residential areas (Table 1 and SI Appendix Fig. S2).

2.2. Geospatial data

Daytime (~11am-1pm) and nighttime (~11pm-1am) Land Surface Temperature (LST_{day} and LST_{night}, respectively) was measured under clear skies during a heatwave on 9-10^{th} February 2017 (Fig. 2); the fourth hottest day and the second hottest night recorded during the 2016/2017 austral summer. LST was measured using an A615 thermal imager (FLIR Systems, Inc., Wilsonville, OR, USA) installed on a Diamond HK36TTC ECO-Dimonas aircraft. LST data (2 m ground resolution) was collected during two dedicated flights at a cruising altitude of 3,000 m (Fig. 1). Flights were kept on stand-by for several days until a suitable heatwave originated; during three consecutive days with daytime maximum air temperature equal or above 40 ℃ in the middle of the study area (Feb 8^{th} = 42.4 ℃; 9^{th} 41.0 ℃; 10^{th} 40.0 ℃ recorded at Adelaide's Kent Town weather station n.23090 (Bureau of Meterology, 2019). Daytime air temperatures during the heatwave were more than 10 ℃ higher than the historical average maximum air temperature recorded in February (1977–2020) at this location.

During the daytime flight, imagery in the red and near-infrared spectra (0.39 m ground resolution) was collected with NIR-modified

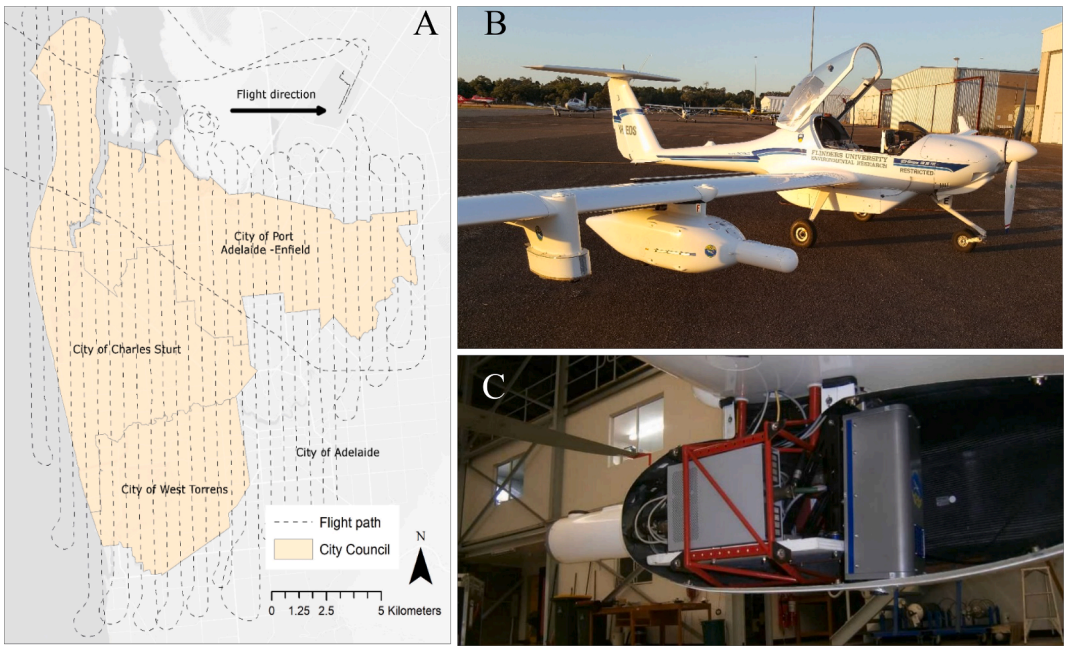

Fig. 1. (A) Map of the study area covering three municipalities and 90 suburbs in western Adelaide, Australia, which encompasses the most frequent land uses and climatic conditions found across the greater metropolitan area (see detailed map in SI Appendix). The size of the area exceeds 149 km^2. The dashed-line indicates the flight path used to measure land surface temperature (LST_{day}, LST_{night}) and collect daytime red and near-infrared imagery (R, NIR). (B) Detail of the Diamond HK36TTC ECO-Dimonas aircraft and the (C) instrument pod fitted with thermal and R-NIR sensors. Flights were kept on stand-by for several days until a suitable heatwave originated (third consecutive day with daytime air temperature $\geq$ 40 ℃ recorded at the Bureau of Meteorology's weather station n.23090 Adelaide's Kent Town, which is more than 10 C higher than the average maximum temperature for February (29.5 C) recorded since 1977 (Bureau of Meterology, 2019). (For interpretation of the references to colour in this figure legend, the reader is referred to the web version of this article.)

Table 1
Land unit class absolute and relative areal coverage within the study area, as well as absolute and relative vegetation (i.e., tree canopy and herbaceous cover) cover within each land unit class. Classes highlighted in light grey represent residential land use. "Other residential" comprises residential buildings other than family houses for which is not possile to locate backyards, corner- or front-yards (e.g., apartment block, condominiums, residential communities, etc.). The number of back and front yards is not the same because some residential parcels do not have paired yards (5).

Land unit class	N. land units	% land units	Total area land units (m^2)	Percent cover unit class (%)	Tree canopy area (m^2)	Herbaceous area (m^2)	Tree canopy cover (% land unit class)	Herbaceous cover (% land unit class)	Tree canopy cover (% total tree cover)	Herbaceous cover (% total herbaceous cover)
Open space	1923	0.62	14,480,873	10.07	2,890,159	6,570,557	19.96	45.37	14.90	28.42
Backyard	64,926	20.92	13,512,690	9.39	4,512,618	3,803,259	33.40	28.15	23.26	16.45
Corner yard	15,065	4.86	4,477,077	3.11	1,317,747	1,251,686	29.43	27.96	6.79	5.41
Front yard	64,654	20.84	9,127,034	6.35	2,184,998	2,411,899	23.94	26.43	11.26	10.43
Other residential	17,152	5.53	3,260,290	2.27	734,037	643,363	22.51	19.73	3.78	2.78
Building	126,594	40.80	33,804,877	23.50	44,243	32,537	0.13	0.10	0.23	0.14
Commercial	5996	1.93	7,011,305	4.87	649,437	465,067	9.26	6.63	3.35	2.01
Industrial	1681	0.54	4,232,054	2.94	328,886	270,908	7.77	6.40	1.70	1.17
Infrastructure	2468	0.80	35,555,375	24.72	4,672,253	4,120,763	13.14	11.59	24.08	17.82
Mixed use	1145	0.37	3,347,044	2.33	634,790	999,583	18.97	29.86	3.27	4.32
Other land use	5982	1.93	6,687,532	4.65	919,195	960,454	13.74	14.36	4.74	4.15
Vacant	2712	0.87	8,013,203	5.57	514,591	1,591,149	6.42	19.86	2.65	6.88
Total	310,298	100.00	143,509,354	99.77	19,402,955	23,121,226	13.52	16.11	100.00	100.00

Canon EOS 6D DSLR camera (Canon, Tokyo, Japan). High-resolution orthorectified cloud-free imagery in the visible spectrum (0.29 m ground resolution, Fig. 2A) and LiDAR point cloud data (average point spacing = 0.8 pts m^{-2}) were obtained for the study area (details in SI Appendix Table S1). Roof footprints of the 156,053 buildings in the study area were obtained alongside a land use map, road network geometry and cadastral data (details in SI Appendix Table S1).

2.3. Geospatial analyses

Geospatial analyses were performed in ArcGIS Desktop 10.6.0.8321 (ESRI, Redlands, CA, USA) and followed the data processing and analysis workflow presented in *SI Appendix – Figure S1*. Briefly, Normalised Difference Vegetation Index (NDVI) was calculated from the red and near-infrared imagery collected from the aircraft. A digital surface model (DSM, 1 m resolution), measuring the height from the ground of all urban features (e.g., buildings, trees, etc.), was calculated from the LiDAR data. A vegetation map detailing tree canopy and herbaceous cover (0.29 m ground resolution, Fig. 2B) was modelled from RGB, NDVI and DSM by using a segmentation and supervised classification approach (methodological details and accuracy assessment are provided in SI Appendix). The land surface temperature differential between day

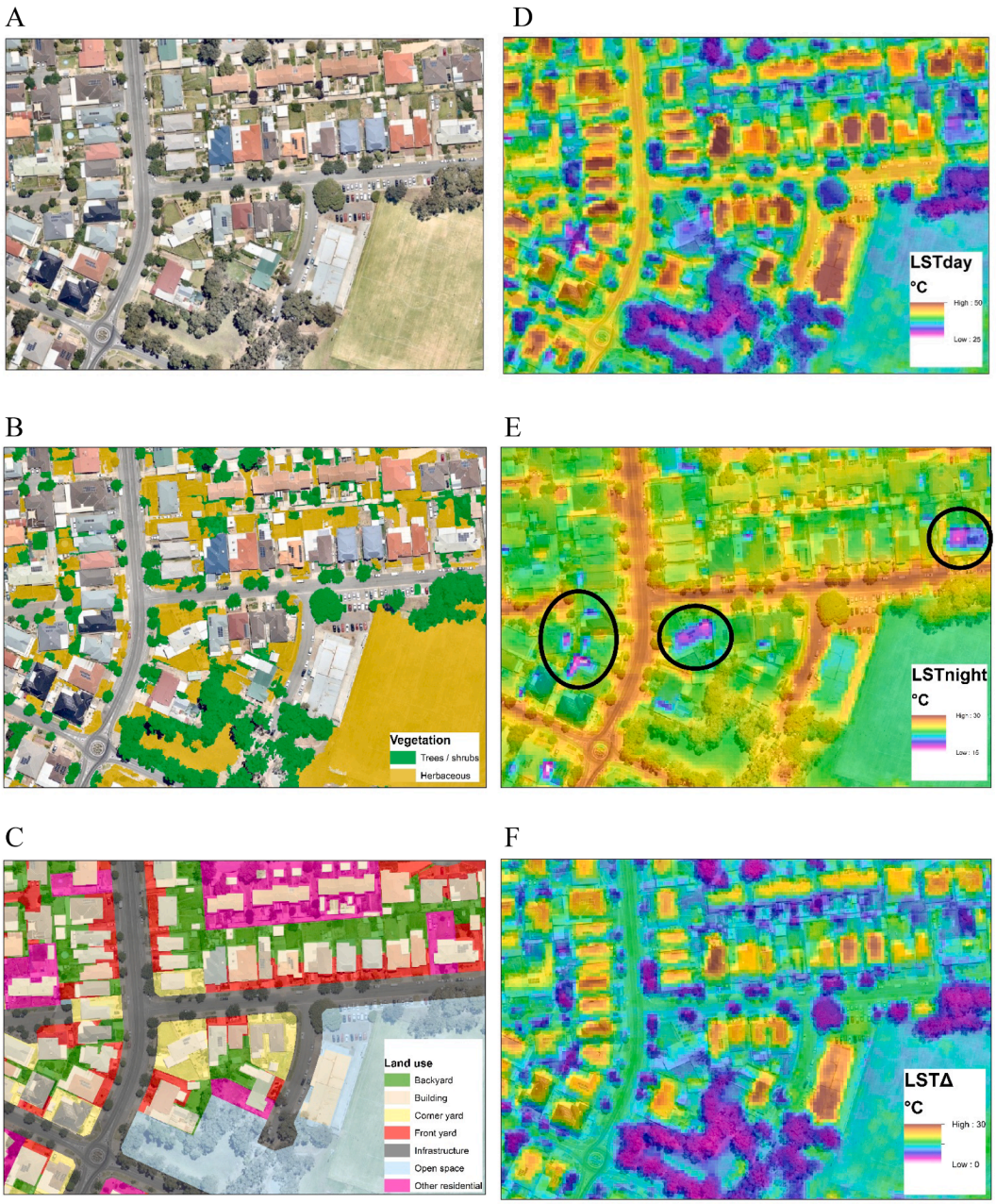

Fig. 2. (A) Detail of the suburb of Ferryden Park in Adelaide, Australia; (B) vegetation map highlighting woody (trees, shrubs) and herbaceous cover; (C) land unit classes; LST_{day} (D), LST_{night} (E) and temperature differential LST_{Δ} (F) collected during a heatwave in the austral summer 2017 (9-10th February). All land unit classes found in the larger study area are listed in Table 1. Black circles in (E) highlight an example of poorly insulated buildings that were likely air-conditioned at night. Maps of LST_{day}, LST_{night} and land use for the entire study area are provided in the SI Appendix.

and night was calculated as $LST_{\Delta} = LST_{day} - LST_{night}$.

As residential yards contain substantial amounts of urban vegetation (Ossola et al., 2019a), all yards were located and classified as either front-, corner- or backyards (Fig. 2C) by using the building footprint, road geometry and parcel cadastral data (Ossola et al., 2019a) (methodological details and accuracy assessment are provided in SI Appendix). LST, distance from the coast, land use fractional composition and vegetation cover data were averaged at two spatial scales: i) at the landscape scale, within each of the 90 suburbs across the study area (average size of 1.66 ± 0.14 (standard error) km^2), and ii) at the local scale, within each of the 310,298 land units (average size of 462.49 ± 8.42 (standard error) m^2) within the study area (Fig. 2C), classified into each of 12 land use classes (see Table 1 and 2). Because vegetation cover around land units has been shown to locally affect urban air temperature within suburbs (Ziter et al., 2019), we further calculated i) the percent cover of tree canopy and ii) the herbaceous vegetation cover within three concentric buffers extending outwards from the perimeter of each land unit (0–30 m, 0–60 m and 0–90 m) for a total of 930,894 buffers (see inset in Fig. 5).

2.4. Data analysis

Statistical analyses aimed to predict LST_{day} LST_{night}, and LST_{Δ} were performed at both suburb and land unit level to investigate factors affecting LST at different spatial scales as well as its diel variation during a heatwave event. Statistical analyses were performed in R 3.6.1 (R Core Team, 2017).

At the suburb scale, generalised linear models (GLMs) were fitted to

Table 2
Summary statistics for Generalised Linear Models (GLMs) predicting average urban land surface temperatures (LST_{day}, LST_{night} and LST_{Δ}) at suburb level (n = 90) based on distance from the coast, vegetation cover and land use predictor variables averaged for each suburb to calculate the respective proportional cover. Coefficient estimates and (standard error) for each predictor are reported in bold at significance levels of *** P < 0.001, ** P < 0.01, and * P < 0.05. "*Front yard cover*", "*Back yard cover*", "*Non-vegetated cover*" and "*Other land use cover*" cover have been excluded from GLMs as they are multi-collinear with the other land cover and land use variables. A complete list of land use classes and their total proportional coverage across the entire study area is provided in Table 1. A correlation matrix for predictors is included in Table S2.

Response variable	LST_{day}	LST_{night}	LST_{Δ}
Null deviance	232.618	12.610	261.663
Residual deviance	49.264	10.160	65.607
R^2	0.788	0.194	0.749
AIC	229.17	87.088	254.96
Predictor variables			
Distance from coast (m)	**0.0004 (0.00005)****	−0.00003 (0.00002)	**0.0004 (0.00006)****
Tree canopy cover (%)	−0.03 (0.038)	−0.021 (0.018)	−0.010 (0.044)
Herbaceous cover (%)	0.041 (0.024)	−0.013 (0.011)	**0.053 (0.027)***
Building cover (%)	0.058 (0.031)	−0.003 (0.014)	0.061 (0.036)
Commercial land cover (%)	**0.100 (0.029)****	−0.007 (0.013)	**0.108 (0.033)****
Corner yard cover (%)	**0.201 (0.103)***	0.048 (0.045)	0.153 (0.119)
Industrial land cover (%)	**0.130 (0.037)****	−0.029 (0.017)	**0.160 (0.044)****
Infrastructure cover (%)	**0.079 (0.019)****	0.002 (0.009)	**0.077 (0.023)****
Mixed use cover (%)	0.046 (0.028)	0.005 (0.013)	0.042 (0.032)
Open space cover (%)	−0.019 (0.021)	−0.006 (0.009)	−0.014 (0.024)
Other residential land cover (%)	**0.154 (0.057)****	**−0.056 (0.026)***	**0.209 (0.065)****
Vacant land cover (%)	0.029 (0.033)	−0.013 (0.015)	0.042 (0.038)

each of the three LST metrics (LST_{day}, LST_{night}, LST_{Δ}) by using predictors previously reported to affect urban LST at the city or neighborhood scale, namely: i) average distance of suburbs from the coast, as inland suburbs are often hotter than coastal suburbs due to reduced sea breezes and increased warm air from inland areas (Khan et al., 2021; Tayyebi and Jenerette, 2016, 2018); ii) urban forest fractional cover (i.e., percent tree canopy and herbaceous cover) , as greener suburbs are often cooler than those with lower vegetation cover (Myint et al., 2013); and iii) land use fractional composition (i.e., percent cover of the main land uses across the study area, see Table 1), as land uses with greater built-up areas and impervious surfaces are generally hotter than less developed suburbs (Soltani and Sharifi, 2017). Prior to modelling, LSTs suburb-level data was modelled to a number of statistical distributions to find the optimal function fitting the data that was used to specify the family of GLMs (i.e., Gaussian) and multi-collinear variables were excluded based on Variable Inflation Factors (VIF). Post-modelling, GLMs were checked for distribution of residuals and model fit.

At the land unit scale, distributed random forest models (DRFs) were fitted to predict the land unit variation of each of LST_{day}, LST_{night}, and LST_{Δ}. DRF modelling is an increasingly popular machine learning technique based on the analysis of multiple regression trees (i.e., random forest) fitted on randomised subsets of predictors and observations (Prasad et al., 2006). DRF was selected over other regression techniques (e.g., GLM) to model LST at the land unit scale as it is i) suitable for big data models performed on highly-dimensional datasets and large numbers of observations (i.e., 27 predictors and 310,298 land units in this instance), ii) capable of handling multicollinear predictors regardless of their statistical distribution, and iii) suitable for modelling datasets with a high number of categorical variables (i.e., suburb identity and the 12 land unit classes coded as dummy variables in this instance). Further, DRF models tend to reduce bias and data overfit (Prasad et al., 2006), despite being computationally demanding. DFR modelling was performed in a cloud-based platform (H2O.ai, 2018, version 3.20.0.2) that can be interfaced to R 3.6.1 (R Core Team, 2017). First, each of the LST_{day}, LST_{night}, and LST_{Δ} datasets were randomly divided into a training and a validation dataset (80% and 20% of land units, respectively). For each LST metric, a DRF model was fitted to the respective training dataset by allowing the algorithm to generate a maximum of 200 statistical trees (max depth = 30) in a 5-fold cross validation fashion. Each model was then tested against each validation dataset to ensure convergence in residual deviance. Predictor variable responses were calculated by using the libraries *DALEX*, *breakDown* and *pdp* in R 3.6.1 (R Core Team, 2017). Predictive performance of DRF model was evaluated by calculating Mean Absolute Error (MAE) and Root Mean Square Error (RMSE) (Ameer et al., 2019).

Predictors used in DRF modelling at land unit scale were those used in suburb-level GLMs but averaged for each land unit. Urban forest fractional cover (i.e., percent tree canopy and herbaceous cover) was averaged within each of the 310,298 land units and to which land use class was also assigned. The composition of the urban forest around land units within three concentric buffers (0–30 m, 0–60 m and 0–90 m) was used as a predictor to account for local effects of vegetated patches upon LST (Ziter et al., 2019). Distance from the coast, suburb identity and land unit area were further included as covariates in the DRF models to account for i) the potential coastal effect on LST as highlighted from the previous suburb-level GLMs and other studies (Tayyebi and Jenerette, 2016, 2018), ii) the possible autocorrelation of vegetation characteristics within the same suburb due to socio-economic characteristics (Ossola and Hopton, 2018), and iii) the fact that urban vegetated cover is generally constrained by the available planting space as dictated by urban morphology (Bigsby et al., 2014).

3. Results

Despite covering only 18.85% of urban land across the 90 suburbs in Adelaide, residential backyards, front yards and corner yards (n = 126,594) contained 41.31% and 32.29% of tree canopy and herbaceous cover, respectively (Table 1). Backyards were the most common green space type across the study area (n = 64,926), with notably higher canopy cover (23.26%) than open space and urban parks (14.90%, n = 1,923). Buildings were the single most abundant land unit (n = 126,594), covering 23.50% of the study area (Table 1).

At the suburb scale, the General Linear Model (GLM) predicting LST_{night} had a much lower model fit (R^2 = 0.205) than those predicting LST_{day} and LST_{Δ} based on the same predictors (R^2 = 0.802 and 0.757, respectively). Diurnal LST variation across the 90 suburbs (mean = 38.46 ℃ ± 4.48 SD, min = 33.70 ℃, max = 41.07 ℃) was greater than the nocturnal temperature variation (mean = 24.82 ℃ ± 2.12 SD, min = 23.66 ℃, max = 25.72 ℃). Suburb-level LST_{Δ} showed similar variation patterns to LST_{day} (Fig. 3A). Suburb-level GLM analyses showed that distance from the coast had the greatest effect on LST_{day} and LST_{Δ} compared to the other predictors, but not on LST_{night} (Table 2). LST_{day} and LST_{Δ} steeply increased from the maritime coastline to about 4 km inland, stabilizing between 4 and 6 km, to then increase again further inland (Fig. 3A). GLMs showed that suburbs with high coverage of impervious land uses, such as commercial and industrial land and infrastructures, had higher LST_{day} and LST_{Δ} compared to other suburbs. Tree canopy cover had no effect on LSTs at the suburb scale, and only herbaceous cover had a marginally significant effect on LST_{day} and LST_{Δ} (Table 2, SI Appendix Fig. 1).

At the land unit scale, Distributed Random Forest (DRF) models predicting LST_{day}, LST_{night} and LST_{Δ} explained about half of initial deviance for the 310,298 land units analysed (Fig. 4). The location of each land unit, based on its suburb and distance from the coast, was one of the most important factors affecting local LST overall (Fig. 4). The land use class of each land unit was the least important factor affecting local LST (Fig. 4, SI Appendix Fig. 2), with the exception of buildings in the DRF models predicting LST_{night} and LST_{Δ}. Overall, the percentage of non-vegetated and vegetated cover (i.e., tree canopy and herbaceous)

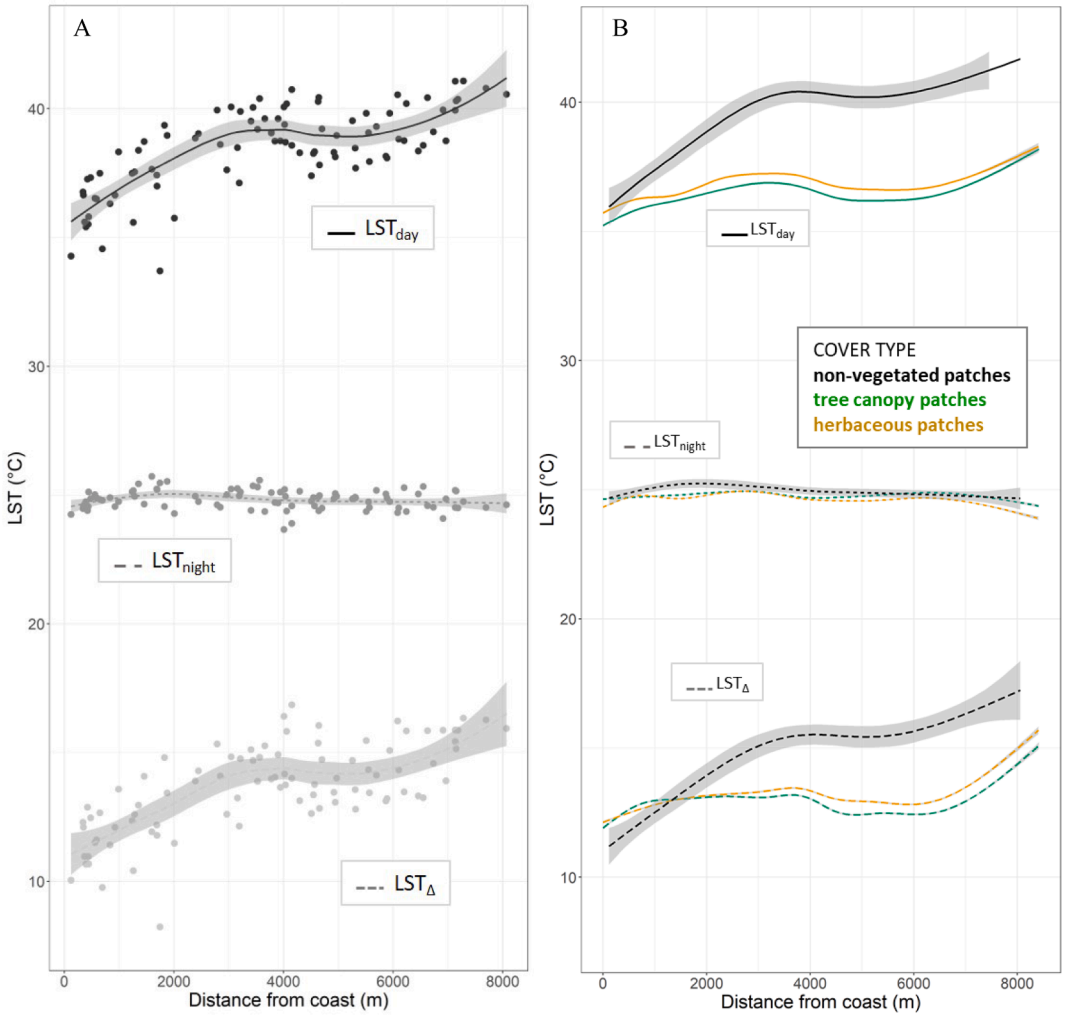

Fig. 3. (A) Urban land surface temperature (LST) recorded during day-, night-time and their differential (LST$_{\Delta}$) as measured across western Adelaide's suburbs (n = 90) in relation to the average distance of each suburb from the maritime coastline. (B) Patch-level surface temperature in relation to distance from the maritime coast. LST$_{day}$ (top), LST$_{night}$ (middle) and LST$_{\Delta}$ (bottom) is averaged across non-vegetated patches, tree canopy (n = 347,485) and herbaceous patches (n = 334,737) regardless of their distribution within the 12 land use classes (Table 1). Points in 3B are omitted for clarity. Lines represent loess models and grey bands the respective confidence intervals.

within each land unit and in the immediate landscape around each unit had high importance in explaining LST variation across land units (Fig. 4). The non-vegetated and vegetated cover in the landscape buffer extending 30 m outwards from the border of each land unit greatly affected local LST$_{day}$ and LST$_{\Delta}$, and to a lesser extent LST$_{night}$ (Fig. 5). The landscape contribution of vegetated cover at decreasing local LST$_{day}$ and LST$_{\Delta}$ decreased with the distance from each land unit. Similarly, the landscape contribution of non-vegetated cover at increasing local LST$_{day}$ and LST$_{\Delta}$ decreased with the distance from each land unit (Fig. 5). Overall, local metrics of vegetation cover were amongst the most important factors affecting LST in all DRF models (Fig. 4).

4. Discussion

4.1. Extreme urban heat across spatial scales

At both the suburb and land unit scale (i.e., local scale), LST$_{day}$ and LST$_{\Delta}$ had a greater variation across the study area than LST$_{night}$. LST$_{\Delta}$ largely reflected differences in LST$_{day}$ rather than LST$_{night}$ (Fig. 3A, Fig. 5). LST$_{night}$ had lower variation across suburbs (23.66–25.72 ℃, min–max) and local land units (10.22–37.46 ℃) compared to LST$_{day}$ (33.70–41.08 ℃ and 15.20–54.75 ℃ for suburbs and land units, respectively). Local LST$_{day}$ and LST$_{night}$ maxima were 13.67 and 11.76 ℃ higher compared to suburb-level maxima. Thus, surface temperatures experienced locally can be up to 25–30% higher compared to those recorded at larger scales. After sunset, the urban land surface has a negative net radiation balance and rapidly re-emits heat toward the atmosphere as long-wave radiation (Bonan, 2000). Because the night flight was performed four to six hours after the civil sunset (19:16 ACDT, Australian Government, Geoscience Australia, http://www.ga.gov.au/geodesy/astro/sunrise.jsp, accessed on 30.11.2019), sufficient time might have occurred to allow most of the heat to dissipate from the urban surface, thus determining the relatively small variation range in LST$_{night}$ we measured. Recent LST measurements at large spatial scales similarly found large variability in LST day-night pairs (Buyantuyev and Wu, 2010; Myint et al., 2013). Fine-scale and repeated diel LST measurements, attempted only at the suburb scale to date (Tayyebi and Jenerette, 2018), will allow further calculation of fine-scale heating and cooling rates for urban features and covers while accounting for seasonality, weather extremes and spatial autocorrelation of thermal properties, not investigated in our study.

Overall, both GLM and DRF models predicting LST$_{day}$ and LST$_{\Delta}$ at suburb and land unit scale were more accurate than those predicting LST$_{night}$. Land use composition and its fractional cover had little effect in

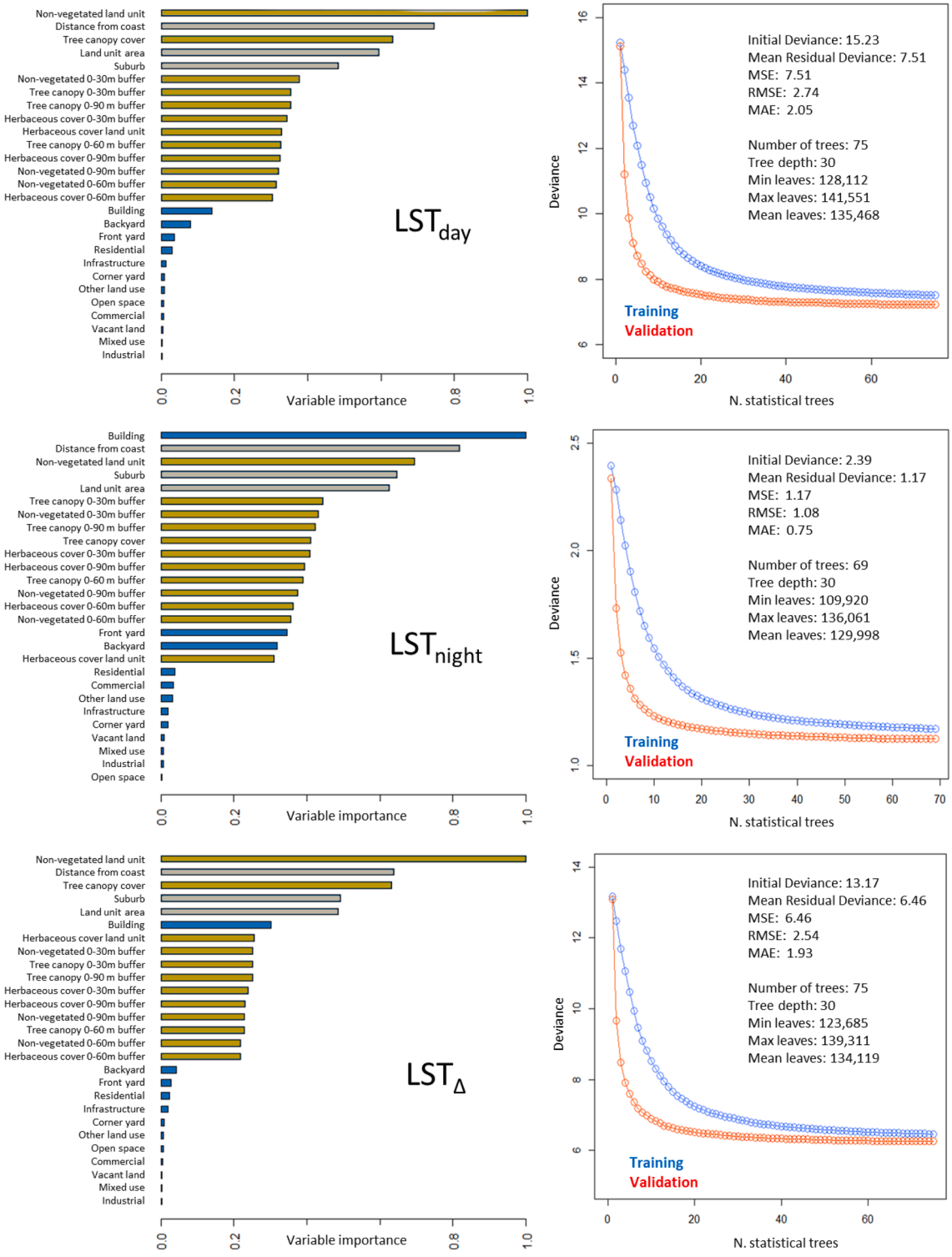

Fig. 4. Variable importance in each of the DRF models predicting LST_{day} (top), LST_{night} (middle) and LST_{Δ} (bottom) based on vegetated and non-vegetated cover within and around each land unit (i.e., 0–30, 0–60 and 0–90 m buffers) (beige bars), land use class of each land unit (blue bars) and location and size of each land unit (grey bars). Line graphs represent the convergence of residual deviance based on the number of statistical trees fitted using the respective training (blue line) and validation datasets (red line). Summary statistics for each DRF model are provided within each line plot. (For interpretation of the references to colour in this figure legend, the reader is referred to the web version of this article.)

the GLM predicting LST_{night} at suburb level (Table 2). Similarly, the use class of each land unit had the lowest importance in the DRF predicting LST_{night} at the local scale (Fig. 4). This suggests that the capacity of an urban area to retain extreme heat at night, at both local and suburb scale, might be less affected by land use, as compared to the capacity of the same area to accumulate heat during the day. In this way, urban land use modifications across scales might be more effective in managing peak LST_{day} rather than minimum LST_{night} as noticed elsewhere (Jenerette et al., 2016). Despite the relatively small difference in LST_{night} across land uses, residential areas overall had the lowest average

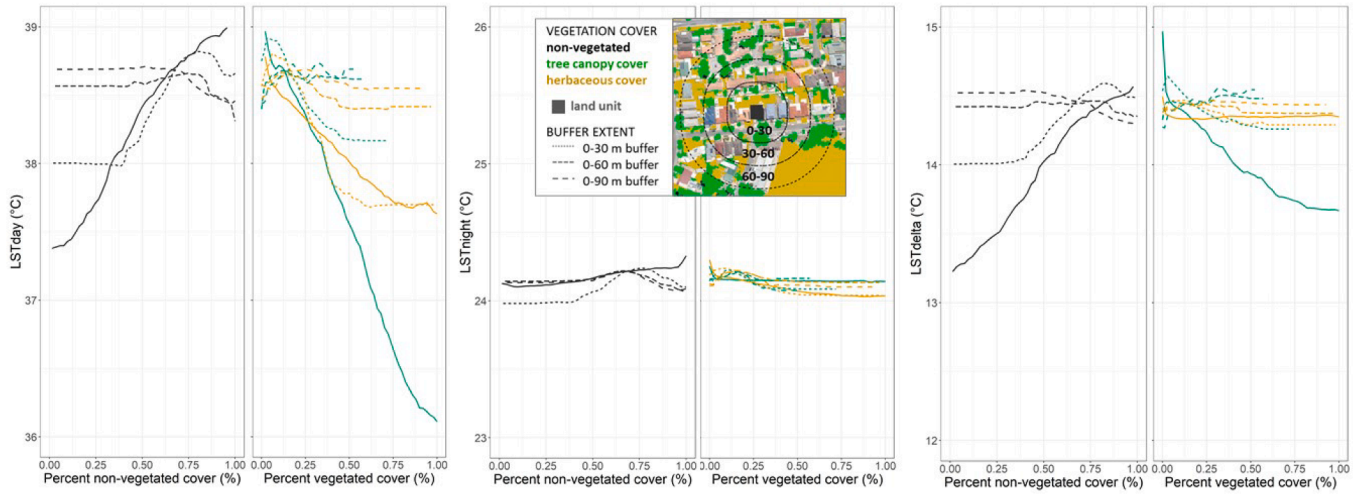

Fig. 5. Response of variables related to vegetated cover (tree canopy in green and herbaceous cover in yellow) and non-vegetated cover (in black) within the 310,298 land units (solid line) and around land units (i.e., 0–30, 0–60 and 0–90 m buffers in dashed lines as per example in the inset) as modelled by using Distributed Random Forest models (DRFs) predicting LST_{day} (left panels), LST_{night} (middle panels) and LST_{Δ} (right panels), respectively. Points and confidence intervals are omitted for clarity. (For interpretation of the references to colour in this figure legend, the reader is referred to the web version of this article.)

LST_{night} suggesting only a slightly reduced human exposure to extreme heat during this period (SI Appendix Fig. 2). Interestingly, several thousand building rooftops were amongst the coolest land units at night (Fig. 2E). This is most likely due to specific building materials or poorly insulated buildings that were intensively air-conditioned during the heatwave, particularly at night when most residents were at home. Thus, other predictors not considered here, such as the type and abundance of materials with different thermal properties, might have also played a role in affecting LST_{night}. At the local land unit scale, the building footprint class was the most important variable in the DRF model predicting LST_{night} (Fig. 4), most likely due to the thermal properties of roofs and greater sky view factors (SVF) able to facilitate heat dissipation after sunset, compared to other urban features. However, percent building cover at the suburb scale was not significant in the GLM predicting LST_{night} (Table 2), as also observed during a dry and hot summer in Phoenix, AZ, USA (Myint et al., 2013).

The fractional cover of several non-residential land uses was a significant factor in the GLM predicting LST_{day} at the suburb level (Table 1), but these were less important in modelling heat at the land unit scale (Fig. 4). This suggests that, moving from the larger urban scale to the local scale, the thermal properties of the materials comprising urban features and covers (e.g., non-vegetated vs vegetated cover) become progressively more important in explaining LST compared to the land uses where these materials are located. For instance, higher infrastructure cover within suburbs determined a higher LST_{day} overall (SI Appendix Fig. 1), but locally this effect might have been negated in instances where streetscapes and other infrastructures were covered by trees (Fig. 5). In this study it was not possible to evaluate the effects of surface albedo and the reflectivity of different materials, despite their importance in affecting LST at various scales (Santamouris et al., 2018).

4.2. Urban heat along the coastal gradient

As expected, a significant coastal gradient affecting extreme urban heat was apparent across the study area at both suburb and land unit scale. As the study area is situated on a flat coastal plain, no interactive effects due to elevation and topography (e.g., aspect) were present. However, the coastal effect moderating LST was significantly lower at night. In fact, the distance from the coast had little effect on LST_{night} at the suburb scale (Fig. 3A), whereas it was retained as the second most important variable in the DFR predicting LST_{night} at local land unit scale (Fig. 4), despite the relatively small range of variation of LST_{night}. On average, suburbs along the coastline were up to 5 ℃ cooler during the day compared to the suburbs furthest from the coast. A study in Los Angeles, CA, USA, a coastal city with comparable climate to Adelaide, similarly found that the diel maximum LST increased by more than 10 ℃ during mild late-spring conditions, but along a coast-inland gradient ten times longer (80 km), also confounded by elevation (Tayyebi and Jenerette, 2018). In Cleveland, OH, USA, a much smaller city along the shore of Lake Erie, a small coastal effect in the moderation of LST was also detected over summer (Declet-Barreto et al., 2016).

The presence of a significant thermal coastal gradient in Adelaide is important, as even small temperature changes of a few degrees, particularly under extreme heat, can have dramatic effects on public health and urban living (Petitti et al., 2016). An analysis of a 14-year hospital admission dataset in Perth, WA, Australia, found a 9.8% increase in daily mortality associated with a 10 ℃ air temperature anomaly during heatwaves (Williams et al., 2012). It remains to be seen to what extent the lower and less variable coastal LST_{Δ} might affect residents' physiological and behavioral adaptation to extreme heat compared to those of inland populations (Hartz et al., 2013). To this point, it is important to note that our findings are based on the assessment of urban land surface temperature rather than air temperature, and as such, not a direct predictor of human thermal comfort. LST, however, might represent a robust indicator when evaluating heat impacts on humans and cities, and for this reason, this parameter has been used in numerous urban epidemiological and climatological studies. For instance, Jenerette et al. (2016) found a strong correlation between LST and self-reported heat illnesses in Phoenix, AZ, US, and in the same city (Harlan et al., 2013) found a positive relationship between heat-related deaths and LST. LST, in fact, is generally well matched to air temperatures measured directly above urban features and covers (Bonan, 2000). LST is also more closely coupled with the thermodynamic properties of land features than air temperature, particularly during daytime, and is a better predictor of biophysical effects on heat, such as transpirational cooling by vegetation (Hulley et al., 2019).

4.3. Urban forest mitigates extreme heat locally

Across the Adelaide suburbs measured, tree canopy and herbaceous cover were relatively low (13.52 and 16.11%, respectively) compared to other urban areas in Australia and globally (Dobbs et al., 2017). Contrary to our expectations, tree canopy cover across suburbs (14.33 ± 3.88% SD) did not significantly affect LST_{day}, even when accounting for

the coastal thermal gradient. Herbaceous cover also had a relatively small effect on decreasing LST_{day}, most likely driven by a few suburbs having herbaceous cover greater than 30% due to the presence of large open green spaces (SI Appendix Fig. S2). LST_{night} was not affected by the local vegetated cover. Ziter et al. (2019) also found a limited effect of local tree cover on air temperature at night in Madison, WI. Other studies in Cleveland, OH and Phoenix, AZ, found small yet significant effects of vegetation cover on LST_{night} at suburb and parcel scale, respectively (Declet-Barreto et al., 2016; Jenerette et al., 2016).

Most previous large-scale assessments found urban vegetation to generally decrease LST_{day} in cities located in different climates and biomes (Declet-Barreto et al., 2016; Myint et al., 2013). The lack of consensus with our findings is likely due to several factors. First, Adelaide's suburbs have a relatively low tree canopy cover compared to neighborhoods in other cities and climates (Ossola and Hopton, 2018). As such, the magnitude of variation range of vegetation cover and LST among studies might have affected this relationship. Second, compared to other cities, Adelaide has a dry summer with low precipitation (64.4 mm (~13% MAP), Dec 2016 - Feb 2017). This affects soil moisture and therefore water available to plants for daytime evapotranspiration, particularly during a heatwave, thus further confounding the relationship between vegetation cover and LST_{day} (Scherrer et al., 2011). As in other studies, we could not account for the effect of irrigation on LSTs (Jenerette et al., 2016, 2011), though the entire state of South Australia is under *Permanent Water Conservation Measures* that have generally limited water use for landscaping since 2003 (Department of Planning and Local Government, 2010). Third, high-resolution studies of urban LST are scant (Bartesaghi-Koc et al., 2019). Prior studies largely investigated LST by using coarse- and medium- resolution thermal sensors (e.g., 7–60 m), and as such a spatial measurement mismatch might be present when comparing these with the fine-scale heat measurements of our study. Prior assessments also largely relied on NDVI datasets rather than more detailed fine-scale maps of canopy and herbaceous covers that better discriminate vegetation features within urban vegetation (Myint et al., 2013; Zhou et al., 2017). In this way, previous evidence captures LST at a resolution unlikely to fully encompass the high thermal variability of urban heat.

At the land unit scale (i.e., tens of meters), however, vegetated cover metrics were amongst the most important factors affecting LST in all DRF models. Ranging from non-vegetated to fully covered land units, trees provided about double the amount of LST_{day} reductions compared to herbaceous vegetation, as observed elsewhere (Jenerette et al., 2016). This also held true when accounting for urban factors known to affect climate and vegetation, such as the coastal thermal gradient and vegetation similarity within suburbs (Cook et al., 2012; Tayyebi and Jenerette, 2016). Contrary to previous evidence (Myint et al., 2013), we did not find any support that herbaceous cover can locally decrease LST_{night} at the land unit scale. This could arise from potentially confounding three-dimensional effects of building walls retarding nocturnal surface radiative cooling at this scale that are not accounted for in our modelling method, which could require further analysis if this is only a nocturnal phenomenon. Our study, however, suggests that herbaceous cover might provide significant benefits by decreasing urban LST_{day} at this scale. This is important because LST_{day} is an important component of urban heating with significant implications for heat vulnerability and public health (Harlan et al., 2006; Jenerette et al., 2016). The thermal benefits of short woody and grassy vegetation are receiving increasing attention alongside those generated by trees (Bartesaghi-Koc et al., 2018). Trees might take decades to grow to maturity and provide heat mitigation, whereas herbaceous cover can be developed quickly and inexpensively. Thus, climate change adaptation strategies to extreme heat events could be geared towards i) short-term localised LST_{day} reductions achieved by using grasses and turf to replace hotter paved and impervious surfaces, integrated with ii) long-term urban forestry strategies aimed at increasing tree cover across cities. In doing so, the selection of grass and turf species having higher water use efficiency and heat tolerance (C4 versus C3 photosynthesis) might also reduce irrigation needs and improve water sustainability in times of scarcity.

LST_{day} of vegetated patches, comparable to that of non-vegetated patches along the coastline, increased proportionally less moving inland. The presence of local tree and grass patches notably "*flattened*" the LST coastal gradient (Fig. 3B), as also observed at a city-wide scale across Los Angeles, CA (Tayyebi and Jenerette, 2018). As such, interventions aimed at mitigating urban heat by using urban green infrastructures, urban forests, etc., are likely to have a greater effect in hotter urban landscapes and hotspots (Jenerette et al., 2016), where significant temperature decreases are also needed the most, particularly under extreme heat and climatic change.

The amount of vegetated cover in the landscape around each land unit also had an effect on LST, particularly during the daytime, although this effect was stronger in the 0–30 m buffer closest to each land unit and tended to saturate when exceeding 50% tree/grass cover in the closest buffer. This is important as it highlights that the overall context of neighborhoods and greening can be designed to locally decrease LST_{day} within each land unit. While a landscape influence on urban air temperature (Ziter et al., 2019) and LST (Yan et al., 2019) has been observed elsewhere, the effect on LST we found is most likely attributable to urban vegetation composition and structure often being more similar within suburbs based on their biophysical characteristics, urban morphology and socio-economics (Ossola and Hopton, 2018) or to the presence of energy exchange across edges of adjacent patches or "*oasis effects*" (Georgescu et al., 2011; Li et al., 2018).

Residential yard presence was not the best DRF predictor of local LST, but yards overall had a proportionally higher tree canopy and herbaceous cover compared to other land unit classes. Yards are often amongst the largest and most widespread land use in some modern western cities, often containing large areas of urban forests (Ossola et al., 2019a, b). However, most current urban greening and forestry strategies and actions are geared towards the public realm (Ossola et al., 2018). Private residential yards represent an untapped opportunity for localised urban heat management and public health benefits. Particular attention will be needed when considering the complex social drivers affecting urban forest and their change. The urban forest in the private realm could be used to locally decrease urban LST by several degrees, particularly where temperature mitigation is needed the most, i.e., closer to homes and residents and when cooling is needed the most, i.e., during periods of extreme heat.

5. Conclusions

Urban heat management currently suffers from a critical mismatch between the scale of urban biophysical properties, such as LST, and the scale of human interventions aimed at mitigating the negative effects of temperature extremes. Because of this, urban governance and planning frameworks hoping to ameliorate and resolve the severe impacts that heatwaves can have on cities, sustainability and public health will need to better value the cooling gains at the urban microclimate level and the local scale (Harlan et al., 2006). Our study is the first to quantify cooling benefits during a heatwave, an extreme weather event that is likely to increase in frequency, intensity and/or duration under climate change. LST reductions, such as those determined by the presence of relatively small and localised tree or grass patches, can be compounded and amplified at larger landscape and city-wide scales. Our overall findings confirm previous evidence about the importance of urban vegetation in reducing LST but further highlight its critical role during extreme weather events such as heatwaves.

Future research could better clarify the effects of urban irrigation on LST, particularly during extreme heatwave events coupled with long-lasting drought, and the concurrent effects due to plant species identity, stomatal conductance, albedo and canopy architecture (e.g., leaf area index, branching). More evidence is also needed to resolve the fine-scale relationships between near-surface air temperatures and LST

across entire urban landscapes under extreme heat, the effects due to spatial autocorrelation of thermal properties and their localised impacts on public health.

This study is amongst the first to suggest the cooling benefits during extreme heat conditions that can be provided by small vegetation patches largely depend on their location within an urban landscape, such as the distance from the coast. Thus, at the *meso*-scale, coastal cities could also prioritise interventions based on larger climatic drivers and physical gradients, such as those arising from the presence of large bodies of water.

Private green spaces, such as people's yards and their trees, are disproportionally important for urban heat mitigation but are currently an overlooked asset for localised climate change adaptation. Managing private green space for urban heat management could help residents to locally adapt to extreme heat when and where this is needed the most; during heatwaves and near home.

Declaration of Competing Interest

The authors declare that they have no known competing financial interests or personal relationships that could have appeared to influence the work reported in this paper.

Acknowledgements

Authors are grateful to Leigh Staas, Jeremy Miller and the municipal councils of the *AdaptWest* consortium; City of Port Adelaide – Enfield, City of Charles Sturt and City of West Torrens for providing data and support to the study. Leanne Hodge, Scott Robinson and Steffen Helgerod provided generous assistance with geospatial data. GDJ is supported by U.S. NSF 1924288.

Appendix A. Supplementary data

Supplementary data to this article can be found online at https://doi.org/10.1016/j.landurbplan.2021.104046.

References

Ameer, S., Shah, M. A., Khan, A., Song, H., Maple, C., Islam, S. U., & Asghar, M. N. (2019). Comparative Analysis of Machine Learning Techniques for Predicting Air Quality in Smart Cities. *IEEE Access, 7*, 128325–128338.

American Meteorological Society. (2020). Glossary of Meteorology Accessed on 23.01.2020 http://glossary.ametsoc.org/wiki/Urban_heat_island.

Australian Bureau of Statistics, 2017, 1270.0.55.003 - Australian Statistical Geography Standard (ASGS): Volume 3 - Non ABS Structures, July 2017. https://www.abs.gov.au/ausstats/abs@.nsf/Lookup/by%20Subject/1270.0.55.003~July%202017~Main%20Features~Overview~1 Accessed on 8.06.2019.

Bartesaghi-Koc, C., Osmond, P., & Peters, A. (2019). Spatio-temporal patterns in green infrastructure as driver of land surface temperature variability: The case of Sydney. *International Journal of Applied Earth Observation and Geoinformation, 83*, Article 101903.

Bartesaghi-Koc, C., Osmond, P., Peters, A., & Irger, M. (2018). Understanding Land Surface Temperature Differences of Local Climate Zones Based on Airborne Remote Sensing Data. *IEEE Journal of Selected Topics in Applied Earth Observations and Remote Sensing, 11*(8), 2724–2730.

Bennett, C. M., Dear, K. B. G., & McMichael, A. J. (2014). Shifts in the seasonal distribution of deaths in Australia, 1968–2007. *International Journal of Biometeorology, 58*(5), 835–842.

Bigsby, K. M., McHale, M. R., & Hess, G. R. (2014). Urban Morphology Drives the Homogenization of Tree Cover in Baltimore. *MD, and Raleigh, NC, Ecosystems, 17*(2), 212–227.

Bonan, G. B. (2000). The microclimates of a suburban Colorado (USA) landscape and implications for planning and design. *Landscape and Urban Planning, 49*, 97–114.

Bowler, D. E., Buyung-Ali, L., Knight, T. M., & Pullin, A. S. (2010). Urban greening to cool towns and cities: A systematic review of the empirical evidence. *Landscape and Urban Planning, 97*(3), 147–155.

Bureau of Meteorology. (2019). Climate statistics for Australian locations accessed on 8.06.2019 http://www.bom.gov.au/climate/averages/tables/cw_023034.shtml.

Bureau of Meterology. (2019). Climate Data Online Accessed on 26/10/2019 http://www.bom.gov.au/climate/data/.

Buyantuyev, A., & Wu, J. (2010). Urban heat islands and landscape heterogeneity: Linking spatiotemporal variations in surface temperatures to land-cover and socioeconomic patterns. *Landscape Ecology, 25*(1), 17–33.

Coates, L., Haynes, K., O'Brien, J., McAneney, J., & de Oliveira, F. D. (2014). Exploring 167 years of vulnerability: An examination of extreme heat events in Australia 1844–2010. *Environmental Science & Policy, 42*, 33–44.

Commonwealth of Australia, B. o. M., 2019, Seasonal Climate Summary for Greater Adelaide - Product code IDCKGC23L0, in: Greater Adelaide in summer 2018–19: warmer and drier than average.

Cook, E. M., Hall, S. J., & Larson, K. L. (2012). Residential landscapes as social-ecological systems: A synthesis of multi-scalar interactions between people and their home environment. *Urban Ecosystems, 15*(1), 19–52.

Cowan, T., Purich, A., Perkins, S., Pezza, A., Boschat, G., & Sadler, K. (2014). More Frequent, Longer, and Hotter Heat Waves for Australia in the Twenty-First Century. *Journal of Climate, 27*(15), 5851–5871.

Declet-Barreto, J., Knowlton, K., Jenerette, G. D., & Buyantuev, A. (2016). Effects of Urban Vegetation on Mitigating Exposure of Vulnerable Populations to Excessive Heat in Cleveland. *Ohio, Weather, Climate, and Society, 8*(4), 507–524.

Department of Planning and Local Government. (2010). *Water Sensitive Urban Design Technical Manual for the Greater Adelaide Region*. Adelaide: Government of South Australia.

Dobbs, C., Nitschke, C., & Kendal, D. (2017). Assessing the drivers shaping global patterns of urban vegetation landscape structure. *Science of The Total Environment, 592*, 171–177.

Dosio, A., Mentaschi, L., Fischer, E. M., & Wyser, K. (2018). Extreme heat waves under 1.5 °C and 2 °C global warming. *Environmental Research Letters, 13*(5), Article 054006.

Gasparrini, A., Guo, Y., Hashizume, M., Lavigne, E., Zanobetti, A., Schwartz, J., Tobias, A., Tong, S., Rocklöv, J., Forsberg, B., Leone, M., De Sario, M., Bell, M. L., Guo, Y.-L. L., Wu, C.-F., Kan, H., Yi, S.-M., de Sousa Zanotti Stagliorio Coelho, M., Saldiva, P. H. N., Honda, Y., Kim, H., & Armstrong, B. (2015). Mortality risk attributable to high and low ambient temperature: a multicountry observational study. *The Lancet, 386*(9991), 369–375.

Georgescu, M., Moustaoui, M., Mahalov, A., & Dudhia, J. (2011). An alternative explanation of the semiarid urban area "oasis effect". *Journal of Geophysical Research: Atmospheres, 116*(D24).

Government of South Australia, 2017, The 30-Year Plan for Greater Adelaide 2017 Update.

Guest, C. S., Willson, K., Woodward, A. J., Hennessy, K., Kalkstein, L. S., Skinner, C., & McMichael, A. J. (1999). Climate and mortality in Australia: Retrospective study, 1979–1990, and predicted impacts in five major cities in 2030. *Climate Research, 13*(1), 1–15.

Harlan, S. L., Brazel, A. J., Prashad, L., Stefanov, W. L., & Larsen, L. (2006). Neighborhood microclimates and vulnerability to heat stress. *Social Science & Medicine, 63*(11), 2847–2863.

Harlan, S. L., Declet-Barreto, J. H., Stefanov, W. L., & Petitti, D. B. (2013). Neighborhood Effects on Heat Deaths: Social and Environmental Predictors of Vulnerability in Maricopa County, Arizona. *Environmental Health Perspectives, 121*(2), 197–204.

Hartz, D. A., Brazel, A. J., & Golden, J. S. (2013). A comparative climate analysis of heat-related emergency 911 dispatches: Chicago, Illinois and Phoenix, Arizona USA 2003 to 2006. *International Journal of Biometeorology, 57*(5), 669–678.

Hulley, G. C., Ghent, D., Göttsche, F. M., Guillevic, P. C., Mildrexler, D. J., & Coll, C. (2019). *3 - Land Surface Temperature* (pp. 57–127). Elsevier.

Imhoff, M. L., Zhang, P., Wolfe, R. E., & Bounoua, L. (2010). Remote sensing of the urban heat island effect across biomes in the continental USA. *Remote Sensing of Environment, 114*(3), 504–513.

IPCC, 2018, Global Warming of 1.5°C. An IPCC Special Report on the impacts of global warming of 1.5°C above pre-industrial levels and related global greenhouse gas emission pathways, in the context of strengthening the global response to the threat of climate change, sustainable development, and efforts to eradicate poverty.

Jenerette, G. D., Harlan, S. L., Buyantuev, A., Stefanov, W. L., Declet-Barreto, J., Ruddell, B. L., … Li, X. (2016). Micro-scale urban surface temperatures are related to land-cover features and residential heat related health impacts in Phoenix, AZ USA. *Landscape Ecology, 31*(4), 745–760.

Jenerette, G. D., Harlan, S. L., Stefanov, W. L., & Martin, C. A. (2011). Ecosystem services and urban heat riskscape moderation: Water, green spaces, and social inequality in Phoenix, USA. *Ecological Applications, 21*(7), 2637–2651.

Khan, H. S., Santamouris, M., Paolini, R., Caccetta, P., & Kassomenos, P. (2021). Analyzing the local and climatic conditions affecting the urban overheating magnitude during the Heatwaves (HWs) in a coastal city: A case study of the greater Sydney region. *Science of The Total Environment, 755*, Article 142515.

Lewis, S. C., King, A. D., & Mitchell, D. M. (2017). Australia's Unprecedented Future Temperature Extremes Under Paris Limits to Warming. *Geophysical Research Letters, 44*(19), 9947–9956.

Li, Y., Kang, W., Han, Y., & Song, Y. (2018). Spatial and temporal patterns of microclimates at an urban forest edge and their management implications. *Environmental Monitoring and Assessment, 190*(2), 93.

Longden, T. (2018). Measuring temperature-related mortality using endogenously determined thresholds. *Climatic Change, 150*(3), 343–375.

Manoli, G., Fatichi, S., Schläpfer, M., Yu, K., Crowther, T. W., Meili, N., … Bou-Zeid, E. (2019). Magnitude of urban heat islands largely explained by climate and population. *Nature, 573*(7772), 55–60.

Mildrexler, D. J., Zhao, M., & Running, S. W. (2011). A global comparison between station air temperatures and MODIS land surface temperatures reveals the cooling role of forests. *Journal of Geophysical Research: Biogeosciences, 116*(G3).

Myint, S. W., Wentz, E. A., Brazel, A. J., & Quattrochi, D. A. (2013). The impact of distinct anthropogenic and vegetation features on urban warming. *Landscape Ecology, 28*(5), 959–978.

Nairn, J., & Fawcett, R. (2013). *Defining heatwaves: Heatwave defined as a heat-impact event servicing all community and business sectors in Australia*. The Centre for Australian Weather and Climate Research.

Ogge, M., Browne, B., Hughes, T., 2019, HeatWatch - Extreme Heat in Adelaide, The Australia Institute. Accessed on 27.09.2019 from https://www.tai.org.au/sites/default/files/P666%20Heatwatch%20Adelaide%20%5BWEB%5D%20_0.pdf.

Oke, T. R., Mills, G., Christen, A., & Voogt, J. A. (2017). *Urban Climates*. Cambridge: Cambridge University Press.

Ossola, A., & Hopton, M. E. (2018). Climate differentiates forest structure across a residential macrosystem. *Science of The Total Environment, 639*, 1164–1174.

Ossola, A., Locke, D. H., Lin, B. B., & Minor, E. (2019a). Greening in style: Urban form, architecture and the structure of front and backyard vegetation. *Landscape and Urban Planning, 185*, 141–157.

Ossola, A., Locke, D. H., Lin, B. B., & Minor, E. (2019b). Yards increase forest connectivity in urban landscapes. *Landscape Ecology, 34*, 2935–2948.

Ossola, A., Schifman, L., Herrmann, D. L., Garmestani, A. S., Schwarz, K., & Hopton, M. E. (2018). The Provision of Urban Ecosystem Services Throughout the Private-Social-Public Domain: A Conceptual Framework. *Cities and the Environment (CATE), 11*(1), 5.

Perkins, S. E., & Alexander, L. V. (2012). On the Measurement of Heat Waves. *Journal of Climate, 26*(13), 4500–4517.

Petitti, D. B., Hondula, D. M., Yang, S., Harlan, S. L., & Chowell, G. (2016). Multiple Trigger Points for Quantifying Heat-Health Impacts: New Evidence from a Hot Climate. *Environmental Health Perspectives, 124*(2), 176–183.

Prasad, A. M., Iverson, L. R., & Liaw, A. (2006). Newer Classification and Regression Tree Techniques: Bagging and Random Forests for Ecological Prediction. *Ecosystems, 9*(2), 181–199.

R Core Team, 2017, R: A Language and Environment for Statistical Computing.

Reisinger, A., Kitching, R., Chiew, F., Hughes, L., Newton, P., Schuster, S., Tait, A., Whetton, P., 2015, Chapter 25: Australasia, in: Intergovernmental Panel on Climate Change Fifth Assessment Report, Working Group II, Impacts, Adaptation & Vulnerability (IPCC, ed.), Geneva, Switzerland.

Robine, J.-M., Cheung, S. L. K., Le Roy, S., Van Oyen, H., Griffiths, C., Michel, J.-P., & Herrmann, F. R. (2008). Death toll exceeded 70,000 in Europe during the summer of 2003. *Comptes Rendus Biologies, 331*(2), 171–178.

Rogers, C. D. W., Gallant, A. J. E., & Tapper, N. J. (2018). Is the urban heat island exacerbated during heatwaves in southern Australian cities? *Theoretical and Applied Climatology*.

Santamouris, M., Ban-Weiss, G., Osmond, P., Paolini, R., Synnefa, A., Cartalis, C., … Kolokotsa, D. (2018). Progress in urban greenery mitigation science - assessment methodologies advanced technologies and impact on cities. *Journal of Civil Engineering and Management, 24*(8), 638–671.

Scherrer, D., Bader, M. K.-F., & Körner, C. (2011). Drought-sensitivity ranking of deciduous tree species based on thermal imaging of forest canopies. *Agricultural and Forest Meteorology, 151*(12), 1632–1640.

Shaposhnikov, D., Revich, B., Bellander, T., Bedada, G. B., Bottai, M., Kharkova, T., … Pershagen, G. (2014). Mortality related to air pollution with the moscow heat wave and wildfire of 2010. *Epidemiology (Cambridge, Mass.), 25(3):359–364*.

Soltani, A., & Sharifi, E. (2017). Daily variation of urban heat island effect and its correlations to urban greenery: A case study of Adelaide. *Front. Archit. Res., 6*(4), 529–538.

Steffen, W., Hughes, L., & Perkins, S. (2014). *Heatwaves: Hotter*. More Often, Climate Council of Australia: Longer.

Tayyebi, A., & Jenerette, D. (2016). Increases in the climate change adaption effectiveness and availability of vegetation across a coastal to desert climate gradient in metropolitan Los Angeles. *CA, USA, Science of The Total Environment, 548–549*, 60–71.

Tayyebi, A., & Jenerette, G. D. (2018). Assessing diel urban climate dynamics using a land surface temperature harmonization model. *International Journal of Remote Sensing, 39*(9), 3010–3028.

Threlfall, C., Marzinelli, E. M., Ossola, A., Bugnot, A., Bishop, M., Lowe, L., … Dafforn, K. (2021). Towards cross-realm management of coastal urban ecosystems. *Frontiers in Ecology and the Environment*. in press.

United Nations. (2018). World Urbanization Prospects 2018 accessed on 24.01.2020 https://population.un.org/wup/.

Watts, N., Amann, M., Arnell, N., Ayeb-Karlsson, S., Belesova, K., Berry, H., … Costello, A. (2018). The 2018 report of the Lancet Countdown on health and climate change: Shaping the health of nations for centuries to come. *The Lancet, 392*(10163), 2479–2514.

Williams, S., Nitschke, M., Weinstein, P., Pisaniello, D. L., Parton, K. A., & Bi, P. (2012). The impact of summer temperatures and heatwaves on mortality and morbidity in Perth, Australia 1994–2008. *Environment International, 40*, 33–38.

WMO. (2019a). United In Science Accessed on 26.10.2019 https://public.wmo.int/en/resources/united_in_science.

WMO. (2019b). WMO Provisional Statement on the State of the Global Climate in 2019 Accessed from https://library.wmo.int/index.php?lvl=notice_display&id=21626#.Xlw9FKhLiUk on 2.03.2020.

Yan, J., Zhou, W., & Jenerette, G. D. (2019). Testing an energy exchange and microclimate cooling hypothesis for the effect of vegetation configuration on urban heat. *Agricultural and Forest Meteorology, 279*, Article 107666.

Zhou, W., Wang, J., & Cadenasso, M. L. (2017). Effects of the spatial configuration of trees on urban heat mitigation: A comparative study. *Remote Sensing of Environment, 195*, 1–12.

Ziter, C. D., Pedersen, E. J., Kucharik, C. J., & Turner, M. G. (2019). Scale-dependent interactions between tree canopy cover and impervious surfaces reduce daytime urban heat during summer. *Proceedings of the National Academy of Sciences, 116*(15), 7575.